NOTATION

N, number of cascades; ρ, electrical resistivity, $\Omega\cdot$cm; z, thermoelectric Q-factor parameter, $^\circ K^{-1}$; x, coordinate, cm; $y(x_k^-)$, $y(x_k^+)$, values of the function y(x) immediately to the left and the right of the point x_k, respectively; T, absolute temperature, °K; T_h, T_c, temperatures of the heat-scattering and heat-receptive faces of the cascade unit, °K; δT, temperature jump at the cascade junction, °K; i, electric current density, A/cm^2; q = Q/I, specific heat flux, V; Q, total heat flux in the thermoelement cross section, W; I, electric current, A; $q_{o_m}^k$, $q_{i_m}^k$, mean specific heat fluxes at the cold and hot faces of the k-th cascade, V; Q_c, heat liberated from the object being cooled, W; Q_h, heat transmitted to the surrounding medium, W; $\mu = Q_h/Q_c$; $J = \ln \mu$, functional to be minimized; W, power, W; R_c, electrical resistance of unit area of contact, $\Omega\cdot cm^2$; α_T, heat-transfer coefficient, $W/m^2\cdot K$; Q_T^k, heat inflow to cold face of k-th cascade from the surrounding medium, W; s, junction area, cm^2; l, thermoelement length, cm; F_o, area of external face of substrate being cooled, cm^2; γ, Q-factor reduction parameter. Indices: n, p, electron, hole thermoelement; k, number of cascade.

LITERATURE CITED

1. V. A. Semenyuk, "Cascade thermoelectric cooling unit as an object of optimal control," Inzh.-Fiz. Zh., 47, No. 2, 333-334 (1984).
2. R. Buist and J. Fenton, "Low-power 145°K thermoelectric cooler," in: Electrooptical System Design Conference, Proceedings of Technical Program, Ind. Sci. Conf. Manage., Inc., Chicago, Ill. (1972).
3. R. Marlow and P. B. Click, "Estimating heat loads on multistage thermoelectric heat pumps," in: Proceedings of the Third International Conference on Thermoelectric Energy Conversion, Arlington, Texas, March 22-24, 1978, IEEE, New York (1978).
4. W. M. Yim and A. Amith, "Bi—Sb alloys for magnetothermoelectric and thermomagnetic cooling," Solid-State Electron., 15, 1141-1165 (1972).

NUMERICAL DETERMINATION OF TWO-DIMENSIONAL TEMPERATURE FIELDS IN TRANSPIRATION COOLING

A. V. Kurpatenkov, V. M. Polyaev, and A. L. Sintsov

UDC 536.24

We present a numerical method for solving a wide range of transpiration cooling problems.

It is well known that an analytic calculation of one-dimensional temperature fields in transpiration cooling of a plate with any (linear) boundary conditions reduces to a sequence of standard mathematical operations, and presents no difficulties. However, even for a one-dimensional problem of the transpiration cooling of a cylinder, and especially for two-dimensional problems, analytic solutions exist only in rare special cases. Accordingly, it is clear that a more general study of transpiration cooling processes must be based on a numerical solution of the appropriate equations.

We know of only one paper devoted to a discussion of the numerical solution of a two-dimensional transpiration cooling problem [1]. In constructing an algorithm Koh and Colony [1] employed a discrete Fourier transform. In doing this they essentially used the simplicity of the eigenfunctions of a difference operator along one of the directions. A rather wide range of problems can be solved by using the algorithm described in [1]. The optimum use of the Fourier transform described, for example, in [2] enables one to obtain a rather economical machine realization of the algorithm. However, the algorithm proposed by Koh and Colony [1] has shortcomings. In particular, it cannot be used to solve problems: 1) of once-through cooling of a porous cylinder; 2) with boundary conditions of the third kind along im-

N. E. Bauman Higher Technical School, Moscow.

Translated from Inzhenerno-Fizicheskii Zhurnal, Vol. 47, No. 6, pp. 984-991, December, 1984. Original article submitted July 19, 1983.

0022-0841/84/4706-1459$08.50

permeable walls; 3) with a variable flow rate of the coolant along a permeable wall, and some others.

We propose an algorithm which can be used to solve both the problems named above and a number of others, in particular problems of cooling bodies with a variable porosity and bodies which are surfaces of revolution.

In constructing a difference scheme of the problem we start from the following integral equations, assuming that they are valid for any finite volume V of a porous medium:

$$\int (\mathbf{n}, \mathbf{q})\, dS = \int \{\alpha_V (T - \tau) - q_V\}\, dV, \tag{1}$$

$$-\int (\mathbf{n}, \dot{m})\, c_p \tau dS = \int \{\alpha_V (T - \tau) - q_V\}\, dV, \tag{2}$$

where S is the surface bounding the volume, **n** is the inward normal to the surface, **q** is the heat flux, T and τ are respectively the temperatures of the solid phase and the coolant, α_V is the volumetric heat-transfer coefficient, c_p is the specific heat, m is the specific flow rate of the coolant, q_V is the volumetric heat source strength, and a comma between two vectors indicates their scalar product. We do not discuss the rather subtle questions of the limits of applicability of Eqs. (1) and (2), and assume that two temperatures T and τ are associated with each point of a porous body, and that heat transfer between the phases is adequately described by the right-hand side of Eqs. (1) and (2). We define the vector **q** by the formula

$$\mathbf{q} = -\Lambda \operatorname{grad} T, \tag{3}$$

where Λ is a symmetric positive tensor which depends on the physical and structural characteristics of the porous body. We neglect the thermal conductivity of the fluid phase, and assume that the principal axes of the tensor coincide with the coordinate system, and that the principal values along the axes are λ_x and λ_y.

We construct an algorithm for a cylindrical body whose axis of symmetry coincides with either the X or Y axis. We note that the X axis will always be in the direction of the coolant velocity, and that the Y axis is perpendicular to it. The body extends a distance L along the X axis and H along Y. All the linear dimensions along the X axis are relative to L, and those along Y are relative to H. If the axis of the cylinder coincides with the X axis, we characterize the latter by the radii Y^n and Y^v, equal to $Y^n + 1$; otherwise, we characterize them by the radii X^a and X^b, equal to $X^a + 1$. We note that X^a always corresponds to the entrance surface of the coolant into the porous body, and X^b to the exit surface. The quantities L and H are always positive, while the quantities Y^n and Y^v or X^a and X^b may also be negative. In order to preserve freedom in the choice of the axis of symmetry, we use Y^n, Y^v and X^a, X^b simultaneously. Depending on the axis of symmetry, the corresponding radii in the calculations must be taken infinite (in the program realization this means sufficiently large numbers). It will be clear from the construction of the algorithm what changes must be introduced to take account of variations of the porosity, flow rate, etc.

We introduce criteria which are important for the problem of transpiration cooling (T is the temperature scale):

$$\varkappa = \lambda_x H^2 (\lambda_y L^2)^{-1},\ \nu = \alpha_V H^2 \lambda_y^{-1},\ q_\varkappa = q_V H^2 (\lambda_y T)^{-1},$$

$$\sigma = \alpha_V L (c_p \dot{m})^{-1},\ \pi_\varkappa = \dot{m} c_p H^2 (\lambda_y L)^{-1},\ \pi_x = \dot{m} c_p L \lambda_x^{-1}.$$

We note the equalities $\nu = \sigma\pi_\varkappa$, $\pi_\varkappa = \varkappa\pi_x$.

We cover the plane of the body with a net whose sides are parallel to the X and Y axes. We denote by M the number of points of intersection of the net with the X axis, and by N the number of intersections with the Y axis, and number them in the directions of the respective axes. Then we can associate with each node of the net two integers I and J which are the analogs of the coordinates of the node. We emphasize particularly that I will be the analog of the coordinate along the X axis, and J the analog of the coordinate along Y. We denote by l_I the step of the net along X relative to L, and by h_J the step along Y relative to H. Figure 1 shows an internal node of the net. We obtain the equation relating the temperature at this node to the temperature at the neighboring nodes by applying Eq. (1) to the volume shaded on the figure. As usual, the integrals and derivatives are evaluated by using linear

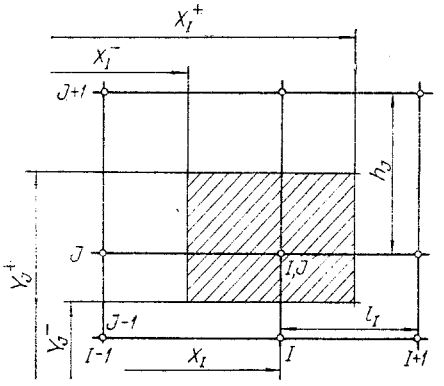

Fig. 1. Net on which the difference approximation of the heat-balance equations is formulated. The heavy lines are the sides of the net, and the points marked are its nodes. The shaded region is the volume for which the approximation is formulated. X_I^-, X_I, and X_I^+ are the radii measured on the X axis, and Y_J^- and Y_J^+ are the radii measured on the Y axis.

interpolation of the temperature between nodes. We expand the left-hand side of (1):

$$\int (\mathbf{n},\ \mathbf{q})\,dS = \int n_x q_x dS + \int n_y q_y dS. \tag{4}$$

The subscripts denote projections on the corresponding axes. We consider first the first term on the right-hand side of (4). Simple transformations give

$$\left(\int n_x q_x dS\right) L^2 (\mathrm{T}\lambda_x V_{IJ})^{-1} \approx Q_{IJ}^x = a_I T_{I-1,J} - b_I T_{IJ} + c_I T_{I+1,J}, \tag{5}$$

$$\left.\begin{aligned} a_I = X_I^- (X_I^0 l_{I-1} l_I^0)^{-1},\ c_I = X_I^+ (X_I^0 l_I^0 l_I)^{-1}, \\ B_I = a_I + c_I,\ l_I^0 = (l_{I-1} + l_I)/2,\ X_I^0 = (X_I^- + X_I^+)/2, \end{aligned}\right\} \tag{6}$$

V_{IJ} is the volume of the region shaded in Fig. 1. It is easy to determine the physical meaning of (5): it is the dimensionless volumetric rate of heat conduction along the X axis. We note that the temperature here and henceforth is relative to the scale T. Relation (5) is valid for the internal nodes of the net. We write an analogous relation for the boundary nodes:

$$\left(\int n_x q_x dS\right) L^2 (\tau\lambda_x V_{1J})^{-1} \approx Q_{1J}^x = -b_1 T_{1J} + c_1 T_{2J} + \omega^a q_{xJ}^a, \tag{7}$$

$$\left(\int n_x q_x dS\right) L^2 (\tau\lambda_x V_{MJ})^{-1} \approx Q_{MJ}^x = a_M T_{M',J} - b_M T_{MJ} - \omega^b q_{xJ}^b, \tag{8}$$

$$\omega^a = X^a (X_1^0 l_1^0)^{-1},\ \omega^b = X^b (X_M^0 l_M^0)^{-1},\ M' = M - 1. \tag{9}$$

In calculating the coefficients a, b, and c with (6) for I = 1, the M quantities a_1, l_0, c_M, and l_M must be set equal to zero, and X_1^- and X_M^+ equated to X^a and X^b, respectively. The last terms in (7) and (8) represent the heat fluxes at the entrance to and exit from the porous body. For them we have the following equations:

$$q_x^a = q_{x\tau}^a + q_{xe}^a,\ q_x^b = q_{x\tau}^b + \beta^b (T^b - \theta^b) + q_{xe}^b. \tag{10}$$

Here the superscript a refers to the entrance to the porous body (the side of the net perpendicular to the X axis, with index I = 1), b refers to the exit, θ^b is the temperature of a certain external flow, $q_{xe}^{a(b)}$ is the X component of the external heat flux supplied to the surface of the body at the coolant entrance (exit), similarly $q_{x\tau}^{a(b)}$ is the X component of the wall–coolant heat flux, β^b is the Biot number, describing the heat exchange with the external flow. The scales used are L, λ_x, and T.

We can obtain expressions similar to (5), (7)-(10) for the second term on the right-hand side of (4):

$$Q_{IJ}^y = A_J T_{I,J-1} - B_J T_{IJ} - C_J T_{I,J+1}, \tag{11}$$

$$Q_{I1}^y = -B_1 T_{I1} + C_1 T_{I2} + \omega^n q_{yI}^n, \tag{12}$$

$$Q_{IN}^y = A_N T_{IN'} - B_N T_{IN} - \omega^v q_{yI}^v, \tag{13}$$

$$\omega^n = Y^n (Y_1^0 h_1^0)^{-1},\ \omega^v = Y^v (Y_N^0 h_N^0)^{-1},\ N' = N - 1,$$

$$q_y^n = \beta^n (\theta^n - T^n) + q_{ye}^n,\ q_y^v = -\beta^v (\theta^v - T^v) + q_{ye}^v. \tag{14}$$

The superscript n refers to the side of the body below the Y axis, and v to the upper side. The remaining notation is analogous to that in (10). It should be kept in mind that here H, λ_y, and T are used as scales. The subscript J in the last terms in (7) and (8) and I

in (12) and (13) mean that the heat flux corresponds to the J-th node on the Y axis in the first case, and to the I-th node on the X axis in the second.

Taking account of the above, Eq. (1) gives for each node of the net:

$$\varkappa Q^x_{IJ} + Q^y_{IJ} = \nu_I(T_{IJ} - \tau_{IJ}) - q_\varkappa. \tag{15}$$

We relate the coolant temperature to that of the solid phase. To do this we apply Eq. (2) to the volume bounded by two neighboring nodes in the direction of the X axis, with a unit side along the Y axis:

$$X_I\tau_I - X_{I-1}\tau_{I-1} = \{\sigma_I(T_I - \tau_I) + \sigma_{I-1}(T_{I-1} - \tau_{I-1})\} X^m l_{I-1}/2. \tag{16}$$

Simple transformations give the following relations:

$$\tau_I = u_{I-1}T_{I-1} + v_{I-1}\tau_{I-1} + w_I T_I, \tag{17}$$

where

$$u_{I-1} = X^m\sigma_{I-1}l_{I-1}\Delta^{-1},\ v_{I-1} = (2X_{I-1} - X^m\sigma_{I-1}l_{I-1})\Delta^{-1},$$
$$w_I = X^m\sigma_I l_I\Delta^{-1},\ \Delta = 2X_I + X^m\sigma_I l_I,\ X^m = (X_{I-1} + X_I)/2.$$

We note that σ_I, like ν_I in (15), denotes the value of the criterion defined at node number I on the X axis.

Formula (17) is valid for the internal nodes of the net. Before deriving the necessary relations for the boundary nodes we note the following. The heat flux from the coolant to the wall at the entrance to or the exit from the body can be defined both in terms of coolant temperatures far from the wall (τ^- at the entrance and τ^+ at the exit) and in terms of a certain mean temperature. In our (linear) case in terms of the arithmetic mean: at the entrance in terms of $\tau^a_m = \frac{1}{2}(\tau^- + \tau^a)$, and at the exit in terms of $\tau^b_m = \frac{1}{2}(\tau^b + \tau^+)$. The choice of the controlling temperature of the coolant is generally arbitrary, and depends on the method of calculating the heat-transfer coefficients α^a at the entrance and α^b at the exit. We use the arithmetic mean temperature of the coolant.

The wall–coolant heat-flux balance at the entrance gives

$$\pi^a_x(\tau^a - \tau^-) = -q^a_{x\tau} = \nu^a(T^a - \tau^a_m),\ \nu^a = \frac{\alpha^a L}{\lambda_x}. \tag{18}$$

Transformations of (18) lead to the following equalities:

$$\tau^a = v_0\tau^- + w_1 T^a,\ -q^a_{x\tau} = \beta^a_\tau(T^a - \tau^-),$$
$$v_0 = (2 - \sigma^a)/(2 + \sigma^a),\ w_1 = 1 - v_0,\ \beta^a_\tau = \pi^a_x w_1, \tag{19}$$
$$\sigma^a = \nu^a/\pi^a_x \text{ is the Stanton number at the entrance.}$$

From the heat-flux balance at the exit

$$\pi^b_x(\tau^+ - \tau^b) = q^b_{x\tau} = \nu^b(T^b - \tau^b_m),\ \nu^b = \frac{\alpha^b L}{\lambda_x},$$

we obtain the formulas

$$\tau^+ = u_M T^b + v_M\tau^b,\ q^b_{x\tau} = \beta^b_\tau(T^b - \tau^b),$$
$$v_M = (2 - \sigma^b)/(2 + \sigma^b),\ u_M = 1 - v_M,\ \beta^b_\tau = \pi^b_x u_M, \tag{20}$$
$$\sigma^b = \nu^b/\pi^b_x.$$

Equations (19) and (20) enable us to extend (17) to the boundary nodes of the net. To do this it is sufficient to take u_0 and w_M equal to zero, and to assume τ_{I-1} equal to τ^- for I = 1, and equal to τ^+ for I = M + 1. The superscript a, as usual, denotes I = 1, and b denotes I = M.

Setting I = 1, 2, ..., M in (17), we obtain a set of formulas, each of which, beginning with the second, contains on the right-hand side the temperature of the coolant determined by the preceding equation. This enables us to derive the following important relation which holds for any I:

$$\tau_I = p_{0,I-1}\tau^- + \sum_{\alpha=1}^{I-1} p_{\alpha+1,I-1}s_\alpha T_\alpha + w_I T_I, \tag{21}$$

$$s_\alpha = u_\alpha + v_\alpha w_\alpha,\ p_{lk} = v_l \cdot v_{l+1} \cdot \ldots \cdot v_k\ (l \leqslant k),\ p_{k+1,k} = 1.$$

In (21), as usual, if the upper index of the sum is smaller than the lower, the sum must be set equal to zero.

Relation (21) enables us to eliminate the coolant temperature from (15), and in this way to obtain a system of linear equations for the T_{IJ}.

We introduce the following notation:

$$\mathbf{T}_J = (T_{1J}, T_{2J}, \ldots, T_{MJ}),\ \tau_J = (\tau_{1J}, \tau_{2J}, \ldots, \tau_{MJ}),$$

and in general we shall use the vector notation to symbolize an ordered set of M quantities defined at the nodes of the net along a single level parallel to the X axis. Then formula (2) can be given the vector form

$$\tau_J = \mathrm{F}\bar{\tau_J} + \mathfrak{P}\mathbf{T}_J, \tag{22}$$

where F is a vector whose I-th component is $p_{0,I-1}$; $\bar{\tau_J}$ is the coolant temperature far from the entrance at the J-th level on the Y axis; $\mathfrak{P}$ is a lower triangular matrix of order M × M, whose I-th row consists of $p_{2,I-1}$, $p_{3,I-1}$, ..., $p_{I,I-1}$, w_I, respectively.

We introduce the M × M matrices $\bar{\mathfrak{N}}$ and $\underline{\mathfrak{N}}$, the first of which has unity in the first place, with the remainder zeros, and the second has unity in the last place, with the remainder zeros, and the vectors $\bar{\mathrm{n}}$ and $\underline{\mathrm{n}}$, the first of which has unity in the first place, with the remainder zeros, and the second has unity in the last place, with the remainder zeros.

The notation introduced enables us to rewrite Eqs. (10) and (14) in vector form:

$$\mathbf{q}_J^a = -\beta_\tau^a \bar{\mathfrak{N}}\mathbf{T}_J + (\beta_\tau^a \bar{\tau_J} + q_{xeJ}^a)\,\bar{\mathrm{n}}, \tag{23}$$

$$\mathbf{q}_J^b = \beta_\Sigma^b \underline{\mathfrak{N}}\mathbf{T}_J - \beta_\tau^b \underline{\mathfrak{N}}\tau_J - (\beta^b\theta^b - q_{xeJ}^b)\,\underline{\mathrm{n}}, \tag{24}$$

$$\mathbf{q}_J^n = \delta_J^n \beta^n \mathbf{T}_J + \delta_J^n (\beta^n\theta^n + \tilde{q}_{ye}^n), \tag{25}$$

$$\mathbf{q}_J^v = \delta_J^v \beta^v \mathbf{T}_J - \delta_J^v (\beta^v\theta^v - q_{ye}^v). \tag{26}$$

Here $\beta_\Sigma^b = \beta^b + \beta_\tau^b$; δ_J^n and δ_J^v are Kronecker deltas, if we keep in mind that n corresponds to J = 1, and v to J = N. In view of this, (25) is different from zero only for J = 1, and (26) is different from zero only for J = N. We denote the last terms in (23), (24), (25), and (26) by $\mathbf{q}_J^{*a}$, $\mathbf{q}_J^{*b}$, $\mathbf{q}_J^{*n}$, and $\mathbf{q}_J^{*v}$, respectively. Now we can write (5)-(8) in the vector form

$$\mathbf{Q}_J^x = \omega^a \mathbf{q}_J^{*a} + (\Omega_\lambda^x - \omega^a\beta_\tau^a\bar{\mathfrak{N}} - \omega^b\underline{\bar{\mathfrak{N}}})\,\mathbf{T}_J + \omega^b\beta_\tau^b\underline{\mathfrak{N}}\tau_J + \omega^b\mathbf{q}_J^{*b}, \tag{27}$$

where Ω_λ^x is a tridiagonal matrix which has $-b_1$, c_1 in the first row, a_2, $-b_2$, c_2 in the second row, ..., a_M, $-b_M$ in the last row. The elements off the three diagonals are zero.

Combining (11)-(13) in vector form gives

$$\mathbf{Q}_J^y = \omega^n \mathbf{q}_J^{*n} + A_J\mathbf{T}_{J-1} - B_J'\mathbf{T}_J + C_J\mathbf{T}_{J+1} + \omega^v\mathbf{q}_J^{*v}, \tag{28}$$

where $B_J' = B_J + \delta_J^n\omega^n\beta^n + \delta^v\omega^v\beta^v$. Substituting (27) and (28) into (15) in vector form, and taking account of (21), we have

$$A_J\mathbf{T}_{J-1} + (\Omega - B_J')\,\mathbf{T}_J + C_J\mathbf{T}_{J+1} = \varphi_J \tag{29}$$

for J = 1, 2, ..., N. We recall that $A_1 = C_N = 0$. We write out all the terms of Eq. (29) in detail:

$$\Omega = \varkappa(\Omega_\lambda^x - \omega^a\beta_\tau^a\bar{\mathfrak{N}} - \omega^b\beta_\Sigma^b\underline{\mathfrak{N}}) - \mathfrak{D}_\nu + \Omega_\tau,$$

$$\Omega_\tau = (\varkappa\omega^b\beta_\tau^b\underline{\mathfrak{N}} + \mathfrak{D}_\nu)\,\mathfrak{P},$$

where $\mathfrak{D}_\nu$ is a diagonal matrix with the diagonal elements ν_1, ..., ν_M. We denote the unit vector by **i**. Then

$$\varphi_J = -\mathbf{q}_J^* - \mathrm{f}\bar{\tau_J} - \mathrm{i}q_\varkappa,$$

where

$$\mathbf{q}_J^* = \varkappa\omega^a\mathbf{q}_J^{*a} + \varkappa\omega^b\mathbf{q}_J^{*b} + \omega^n\mathbf{q}_J^{*n} + \omega^v\mathbf{q}_J^{*v};$$

$$\mathrm{f} = \varkappa\omega^a\beta_\tau^a\bar{\mathrm{n}} + (\varkappa\omega^b\beta_\tau^b\underline{\mathfrak{N}} + \mathfrak{D}_\nu)\,\mathrm{F}.$$

The system (29) is the result of all the preceding calculations. It is the difference approximation of Eqs. (1) and (2) which establish the heat balance within a porous body. As

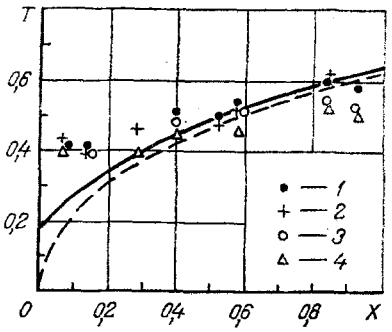

Fig. 2. Comparison of temperature distribution along heated wall measured from the coolant side [3] with the calculated temperature distribution of the coolant (dashed curve) and the porous metal (solid curve). Controlling criteria: $\pi_\varkappa = 2.54$, $\sigma = 10.9$, $\varkappa = 0.0021$. For heat fluxes q supplied to the wall of the inner tube: 1) q = 216 kW/m^2; 2) 261; 3) 341; 4) 420.

regards the boundary conditions, on sides a and b conditions of the second or third kind can be obtained by setting the numbers β or the external-heat fluxes equal to zero in (23) and (24). It is well known that boundary conditions of the first kind can be obtained from those of the third kind by a sufficient increase of the corresponding numbers β. Any combination of boundary conditions is possible. All we have said can be transferred to boundary conditions on sides n and v also.

Turning to the question of the solution of system (29), we note that the use of iterative methods for systems of this type is essentially based on specific properties of them expressed by certain numbers [2]. Obtaining these numbers for system (29) is rather difficult because of the "skewness" introduced into Ω by the Ω_τ matrices. This "abnormality" of the system is a result of the specific process which it describes.

We solve (29) by the explicit matrix pivotal method [2]. The first step consists in evaluating the following matrices and vectors:

$$\mathfrak{A}_J = (\Omega - B_J' - A_J C_{J-1}\mathfrak{A}_{J-1})^{-1},$$

$$\boldsymbol{\beta}_J = \mathfrak{A}_J(\varphi_J - A_J\boldsymbol{\beta}_{J-1}),\ J = 1, 2, \ldots, N.$$

At the second step we calculate T_J:

$$\mathbf{T}_J = -C_J\mathfrak{A}_J\mathbf{T}_{J+1} + \boldsymbol{\beta}_J,\ J = N, N-1, \ldots, 1.$$

The coolant temperature is then determined from (17) by using (19) and (20). The main disadvantage of the pivotal method is the necessity of inverting and storing N matrices of order M × M.

It is not possible in the present article to discuss the analysis of the laws of transpiration cooling processes. However, we illustrate the possibilities of the method described by calculating a problem which was studied experimentally in [3].

The experimental model consisted of two coaxial tubes with the space between them filled with steel shot, apparently sintered. The coolant was gaseous nitrogen. The inner tube was heated by hot gases. Koh and Stevens [3] measured the temperature distribution and the normal heat flux along the wall of the hot tube from the porous metal side. Measurements showed that the heat flux was practically constant along the wall. The temperature distributions were given in [3] for two flow rates of the coolant and a number of heat fluxes.

Let us calculate the temperature field for one of the flow rates. Without going into details, we note that the internal scale of the medium (the equivalent hydraulic diameter in the terminology of [4]) was determined from experimental data in [5], the volumetric heat-transfer coefficient was calculated with formulas given in [4], and λ_x ($=\lambda_y$) was found from the formula recommended in [6]. The value obtained for the thermal conductivity was well correlated with the corresponding experimental value used in [1]. Since the coolant channel is much longer than the internal scale of the porous metal, we neglect heat transfer at the channel entrance and exit. The experimental justification for this possibility was given in [7]. The temperature scale T was defined as qH/λ_y, where q is the dimensional heat flux supplied to the inner tube of the experimental model. It is easy to see that this choice of T guarantees that the dimensionless heat flux q_y^n is independent of variations of q. Accordingly, the calculated dimensionless temperature fields are also independent of q. The "zero" of temperature was taken as the coolant temperature far from the entrance to the porous metal. More concisely, system (29) was solved with the following boundary conditions:

$$\tau^- = 0,\ q_y^n = 1,\ q_y^v = 0,\ q_x^a = q_x^b = 0.$$

Figure 2 shows the results of the calculations. It is clear from the figure that the X dependence of the temperature is weaker for the experimental than for the calculated values. This "averaging" effect is apparently the result of longitudinal heat fluxes in the wall of the inner tube. This effect is particularly noticeable for small X, the region where the coolant enters the porous body, where the longitudinal heat fluxes reach a maximum. In addition, the slope of the experimental curve in the region of the coolant exit from the porous body indicates a definite outflow of heat from the hot end of the tube and the porous metal. The diagram of the experimental model shows that the coolant collector is located here. Taking all this into account, it should be noted that the calculated and experimental values agree rather well. In conclusion we note that calculations performed with the algorithm in [1] do not compare well with experiment, since, as stated previously, that algorithm cannot take account of the axial symmetry of the model.

LITERATURE CITED

1. J. C. Y. Koh and R. Colony, "Analysis of cooling effectiveness for porous material in a coolant pass," Trans. ASME, J. Heat Trans., 96, 324 (1974).
2. A. A. Samarskii and E. S. Nikolaev, Methods of Solution of Net Equations [in Russian], Nauka, Moscow (1978).
3. J. C. Y. Koh and R. L. Stevens, "Enhancement of cooling effectiveness by porous materials in coolant passages," Trans. ASME, J. Heat Trans., 97, 309 (1975).
4. M. É. Aérov and O. M. Todes, Hydraulic and Thermal Principles of Operation of Devices with a Stationary and Fluidized Bed [in Russian], Khimiya, Leningrad (1968).
5. S. V. Belov, G. P. Pavlikhin, and V. S. Spiridonov, "Properties of filtration elements of porous metals," Izv. Vyssh. Uchebn. Zaved., Mashinostr., No. 5, 96 (1978).
6. J. C. Y. Koh and A. Fortini, "Prediction of thermal conductivity and electrical resistivity of porous metallic materials," Int. J. Heat Mass Transfer, 16, 2013 (1973).
7. V. M. Polyaev and A. V. Sukhov, "Investigation of heat transfer in the flow of gas through a porous wall with an internal heat source," Izv. Vyssh. Uchebn. Zaved., Mashinostr., No. 8, 77 (1969).

EFFECT OF IMPURITY ATOMS IN FERROMAGNETS ON MAGNETIC RELAXATION

P. P. Galenko

UDC 621.317.41:538.27

Results are presented from an experimental study of magnetic relaxation in iron specimens containing various amounts of carbon.

A number of studies have been dedicated to time effects in ferromagnets [1-9, et al.]. Study of magnetic relaxation processes in these materials is of great practical significance in connection with their wide use in machine construction, radioelectronics, computer technology, and other fields. The requirements for homogeneity and, especially, time stability of properties being demanded of these materials are increasing continually.

At the present time, according to standard 802-58 [10], in defining the magnetic characteristics of ferromagnetic materials it is necessary to consider the time required for relaxation processes.

One of the manifestations of time effects is a decrease in magnetic permeability of ferromagnets over time after demagnetization by an ac magnetic field of decreasing amplitude. This relaxation phenomenon has been termed magnetic permeability disaccommodation (MPD) and appears especially intensely in iron containing impurity atoms.

The present study is dedicated to an investigation of MPD in iron.

Applied Physics Institute, Academy of Sciences of the Belorussian SSR.

Translated from Inzhenerno-Fizicheskii Zhurnal, Vol. 47, No. 6, pp. 991-995, December, 1984. Original article submitted August 5, 1983.